### Title

Morphometric Analysis of Axons and Dendrites as a Tool for Assessing Neurotoxicity




### ISBN

9781071616369



### Authors

Morgan, Rhianna K
Schmuck, Martin
Grodzki, Ana Cristina
et al.



### Publication Date

2021

### DOI

10.1007/978-1-0716-1637-6_4

Peer reviewed

# Chapter 4

# Morphometric Analysis of Axons and Dendrites as a Tool for Assessing Neurotoxicity

**Rhianna K. Morgan, Martin Schmuck, Ana Cristina Grodzki, Donald A. Bruun, Lauren E. Matelski, and Pamela J. Lein**

## Abstract

Chemical perturbation of the temporal or spatial aspects of axonal or dendritic growth is associated with neurobehavioral deficits in animal models, and structural changes in axons and dendrites are thought to contribute to clinical symptoms associated with diverse neurologic diseases. Consequently, axonal and dendritic morphology are often quantified as functionally relevant endpoints of neurotoxicity. Here, we discuss methods for visualizing and quantifying axonal and dendritic morphology of neurons from the peripheral or central nervous systems in in vitro and ex vivo preparations. These methods include visualization of neuronal cytoarchitecture by immunostaining axon- or dendrite-selective antigens, transfecting cells with cDNA encoding fluorescent proteins, or labeling cells using membrane permeable small molecules that distribute throughout the cytoplasm, Golgi staining or Diolistics, as well as quantifying axonal and dendritic morphology using semi-automated or fully automated image analysis.

**Key words** Automated image analysis, Diolistics, Golgi staining, High-content imaging, Immunocytochemistry, LUHMES cells, Neurite outgrowth, Neurotoxicity, Primary neurons, Sholl analysis

## 1 Introduction

Most neurons in the vertebrate central and peripheral nervous systems extend two types of processes—axons and dendrites—which differ functionally, biochemically, and structurally [1, 2]. The primary function of axons is to convey electrical signals from the neuronal cell body to downstream cells in the neural circuit. Axons typically extend considerable distances from the neuronal cell body to the target tissue, are of uniform caliber throughout most of their length, and are mostly unbranched until they reach the target tissue. In contrast, dendrites comprise the primary site of synaptic input to the neuron. Dendrites are broad at their proximal end and taper over their length to fine distal tips.

Rhianna K. Morgan and Martin Schmuck contributed equally to this work.

Jordi Llorens and Marta Barenys (eds.), *Experimental Neurotoxicology Methods*, Neuromethods, vol. 172,
https://doi.org/10.1007/978-1-0716-1637-6_4, 

Dendrites tend to end proximal to the neuronal cell body and are highly branched throughout their length. Axons and dendrites are collectively referred to as neurites although the term "neurite" is also used to refer to neuronal processes that are not fully differentiated into an axon or dendrite, as occurs during early stages of neuronal differentiation [2], and is often the case with neuronal cell lines [3].

Axonal and dendritic morphology are critical determinants of neuronal function [1]. The shape of these processes affects signal processing within the neuron, while their number, length, and branching patterns determine the pattern of synaptic connections, which in turn regulates the distribution of information within the nervous system. Experimental evidence indicates that even subtle perturbations of temporal or spatial aspects of axonal and dendritic growth can cause persistent changes in synaptic patterning in the developing brain [4–7]. Clinical data confirm that altered axonal and dendritic structure is strongly associated with not only neurodevelopmental disorders but also neurodegenerative diseases [8–13]. Based on such observations, chemical-induced changes in axonal and dendritic morphology are considered functionally relevant endpoints of neurotoxicity [14–16]. Thus, there is considerable interest in using morphometric analysis of axons and dendrites to screen chemicals for neurotoxic potential and to elucidate mechanisms of neurotoxicity. Multiple approaches are used to measure axonal and dendritic morphology, but across all approaches, there are two key steps: (1) visualizing the axonal plexus and/or dendritic arbor of neurons and (2) quantifying axonal and dendritic morphology. Choosing which method to use depends upon the experimental model, e.g., in vitro or ex vivo, and on whether distinguishing between toxic effects on axons vs. dendrites is a desired outcome [17–19]. In this chapter, we present several methods for visualizing and analyzing axonal and dendritic growth of peripheral and central neurons in vitro and ex vivo.

## 2 Materials

### 2.1 Immunocytochemical Approaches for Visualizing Axons and Dendrites In Vitro

To identify axons in primary peripheral neurons, antibodies (Ab) specific for protein gene product 9.5 (PGP9.5, Thermo Fisher Scientific 38–1000/Invitrogen PA110011, RRID:AB_1088162) or the phosphorylated forms of heavy (NF-H) and medium (NF-M) neurofilament subunits (SMI-31; Sternberger Immunocytochemicals/MilliporeSigma NE1022, RRID:AB_2043448) are widely used. For primary central neurons, Ab specific for tau-1 (MilliporeSigma MAB3420, RRID:AB_94855) is used to label axons. To label dendrites in primary neurons from either the peripheral or central nervous system, Ab specific for microtubule-

associated-protein-2 (MAP2) (SMI-52; Sternberger Immunocytochemicals/Synaptic Systems 188 004, RRID:AB_2138181/Invitrogen PA1-10005, RRID:AB_1076848) or non-phosphorylated forms of NF-H and NF-M neurofilament subunits (SMI-32; Sternberger Immunocytochemicals/SigmaAldrich 559844, RRID: AB_2877718) are effective. Additional materials needed include a fixative, usually 4% paraformaldehyde (MilliporeSigma) in 0.1 M phosphate buffer, and a permeabilization buffer [0.1% Triton-X-100 (MilliporeSigma) in phosphate-buffered saline (PBS)] for antibodies to gain access to intracellular antigens. Also needed are a blocking buffer (PBS supplemented with 1–10% bovine serum albumin and/or 1–20% serum of the same species as the host species of the secondary antibody) to decrease binding of antibodies to nonspecific binding sites, fluorophore-tagged secondary antibodies that cross-react with the primary antibodies, and mounting medium [ProLong Gold Antifade Mountant (Invitrogen) for slides].

### 2.2 Transfection of Cultured Neurons with Fluorescent Probes to Visualize Axonal or Dendritic Growth

Primary peripheral and central neurons can be transfected with low efficiency (which is desirable to facilitate visualization of the axonal plexus or dendritic arbor of individual neurons, particularly in high density cultures) using Lipofectamine 2000 (Invitrogen) following the manufacturer's protocol. However, due to cytotoxic effects of lipid transfection reagents on primary neurons, we reduce the incubation time for transfection to only 1–2 h with total replacement of the transfection solution with cell culture media at the end of the incubation period. Dendrites are labeled by transfecting cultures with plasmids encoding microtubule-associated-protein-2B fused to either enhanced green fluorescent protein (MAP2B-eGFP) or red fusion protein (MAP2B-FusRed), which is under the control of the neuron-specific CAG promoter [20]. Expression of these MAP2B fusion proteins is restricted to the somatodendritic compartment in cultured hippocampal neurons and does not alter their intrinsic dendritic growth patterns [20]. To label all processes (dendrites and axons), we transfect neurons with pCAG-tomato fluorescent protein (TFP) constructs. TFP distributes throughout the cytosol and does not alter neuronal morphology. We obtained these plasmids, which are not commercially available, from Dr. Gary Wayman (Washington State University, Pullman, WA, USA).

### 2.3 Live Cell Staining to Visualize All Neurites in the Culture

Calcein-AM (C3100MP, Molecular Probes), a cell-permeant dye used to determine cell viability in eukaryotic cells, will effectively fill all neurites in live cells. In live cells, the non-fluorescent calcein-AM is converted to fluorescent calcein-AM following acetoxymethyl ester hydrolysis by intracellular esterases. The fluorescent calcein-AM can be measured at excitation/emission (ex/em) wavelengths

of 494 and 517 nm, respectively. It is often used in conjunction with Hoechst 33342 (Thermo Fisher Scientific) and propidium iodide (PI; MilliporeSigma). Hoechst 33342 is a cell-permeable DNA stain that is excited by ultraviolet light and emits blue fluorescence at 460–490 nm. It preferentially binds adenine-thymine (A-T) regions of DNA and effectively labels nuclear chromatin. PI labels the nuclear membrane of compromised or dead cells and is used to identify non-viable cells in culture.

### 2.4 Diolistics to Label Processes of Neurons in Peripheral Ganglia or CNS Slice Cultures Ex Vivo

We use the Bio-Rad Helios Gene Gun Low-Pressure system for Diolistics labeling. This all-inclusive system contains a Tubing Prep Station, tubing cutter, cartridge storage vials and extractor tool, tungsten M-25 microcarriers, and Tefzel tubing. Additional supplies needed include polyvinyl pyrrolidone (PVP; MilliporeSigma), methylene chloride (Thermo Fisher Scientific), 1,1′-dioctadecyl-3,3,3′,3′-tetramethylindocarbocyanine perchlorate (DiI) or other similar fluorescent dyes (Molecular Probes), hanging drop slides (Thermo Fisher Scientific), Sylgard 184 (Electron Microscopy Sciences), nitrogen, helium, three-way stopcock, ethanol, razor blades, and 35-mm plastic tissue culture dishes.

### 2.5 Golgi Staining to Visualize Dendrites in Intact Brain Tissue Ex Vivo

We use the FD Rapid GolgiStain kit (FD Neurotechnologies Inc.) for Golgi staining. Materials needed in addition to reagents supplied with this kit include plastic forceps to transfer tissues, plastic scintillation vials for incubation of tissue in Golgi solutions, 60 cm Whatman #1 paper to filter Golgi solutions, as well as standard histological supplies such as microscope coverslips and slides, staining dishes, slide holders, ethanol, chromium potassium sulfate, gelatin, sucrose (MilliporeSigma), and PBS.

## 3 Methods

### 3.1 Visualizing Neurites

Approaches for visualizing neurites include: (1) immunostaining for antigens selectively expressed in axons versus dendrites; (2) expressing cDNA encoding axon or dendrite-selective proteins linked to fluorescent tags or cDNA encoding intracellular fluorescent proteins that distribute throughout the entire cell; and (3) labeling neurons with cytoplasmic dyes or lipophilic membrane dyes (Table 1).

Immunostaining for antigens selectively expressed in axons versus dendrites is most often used to visualize neurites in primary cell culture and offers the advantage of distinguishing axons from dendrites. This method labels all axonal or dendritic processes in the culture. Therefore, in low cell density cultures or at very early times after plating in higher density cultures, this approach can be used to identify processes extended by individual cells.

**Table 1**
**Biomarkers for visualizing neurite outgrowth in vitro and ex vivo within the peripheral and central nervous systems**

| | Axons | Dendrites |
|---|---|---|
| Peripheral nervous system, e.g., postganglionic sympathetic neurons | *In vitro:* ICC analyses of phosphorylated neurofilament (phospho-NF-H and phospho-NF-M) subunits or tau as early as DIV 1 (3–8 cells/mm$^2$) [31] | *In vitro:* ICC analyses of MAP2 or dephosphorylated forms of M and H neurofilament subunits in cultures ≥48 h post-induction of dendritic growth (25,000 cells/cm$^2$) [35, 36] |
| | *Ex vivo:* IHC analyses of phosphorylated neurofilament subunits or tyrosine hydroxylase (TH) in target tissues [72] | *Ex vivo:* Ballistic delivery system of fluorescent dyes (Diolistics) using 1,1′-dioctadecyl-3,3,3′,3′-tetramethyl-indocarbocyanine perchlorate (DiI)-coated tungsten beads [46, 50] |
| Central nervous system, e.g., hippocampal neurons | *In vitro:* ICC analysis of Tau-1 (33,000 cells/cm$^2$) performed at DIV 2 [19] | *In vitro:* MAP2B ICC or pCAG-MAP2B-TFP transfection (83,000 cells/cm$^2$) [19, 20] |
| | *Ex vivo:* "Brainbow" transgenic mice or injection of adenoviral or lentiviral vectors expressing cDNA encoding fluorescent proteins [21–23] | *Ex vivo:* Golgi staining [44] |

*ICC* Immunocytochemistry, *IHC* Immunohistochemistry

Expressing cDNA encoding axon or dendrite-selective proteins linked to fluorescent tags or cDNA encoding intracellular fluorescent proteins that distribute throughout the entire cell are most useful when working with cultures of high cell density or mature cultures with extensive neurite outgrowth. In either case, it is often not possible to distinguish the dendritic arbor or axonal plexus of an individual cell from that of adjacent cells in the culture. The latter challenge can be overcome by using low efficiency transfection to label a small subpopulation of cells in the culture. Similarly, adenoviral or lentiviral infection with cDNA encoding fluorescent proteins can be used to label a subpopulation of neurons in the intact brain although this approach often involves infecting the living animal prior to harvesting of tissue for analysis [21–23].

Labeling neurons with cytoplasmic dyes or lipophilic membrane dyes can be used in vitro or ex vivo. Sometimes, there is incomplete labeling with this approach such that distal ends of processes are not labeled. Most membrane permeant cytoplasmic dyes and lipophilic membrane dyes label all neurites, so distinguishing axons from dendrites is only possible using structural criteria [2], which can be subjective. As with immunocytochemistry, in

high density or mature low density cultures, it is challenging to identify the neurites associated with individual neurons. This issue can be overcome by measuring all neurites in a sample and then dividing by the number of nuclei (usually identified using a nuclear stain, such as Hoechst or DAPI). However, this approach is only feasible when cultures do not contain non-neuronal cells.

Specific examples of these different approaches to visualize neurites are provided below. This is not an inclusive list, but rather a description of methods that have worked well in our hands. While we describe their application using specific models, these methods can be readily adapted to other models.

#### 3.1.1 Visualizing Neurites in the LUHMES Neuronal Cell Line

Neuronal cell lines are significantly easier to obtain and maintain than primary neuronal cell cultures and are particularly useful when large numbers of cultures are needed (e.g., for screening chemical libraries) [24]. The laboratory of Marcel Leist (University of Konstanz, Germany) has championed the use of the human LUHMES (*Lu*nd *H*uman *Mes*encephalic) cell line for neurotoxicity assays [25], and we have successfully used the LUHMES cell line to evaluate the effects of soluble immune mediators on neurite growth and retraction [26]. LUHMES cells were originally derived from 8-week-old female ventral mesencephalon. We obtained this cell line as a generous gift from the Leist laboratory, but LUHMES cells can also be purchased from the American Type Culture Collection (ATCC®; CRL-2927, RRID:CVCL_B056). This cell line is a sub-clone of the tetracycline-controlled, v-myc-overexpressing human mesencephalic-derived cell line MESC2.10 [27]. Like MESC2.10 cells, LUHMES cells can be differentiated into non-mitotic cells that recapitulate the morphological and biochemical characteristics of mature dopaminergic-like neurons by exposing undifferentiated, dividing LUHMES cells to tetracycline, glial cell line-derived neurotrophic factor (GDNF), and dibutyryl 3,5-′-cyclic adenosine monophosphate (db-cAMP).

LUHMES culture and differentiation are described in detail by Scholz and collaborators [3], and the quantification of neurite outgrowth using the Array-Scan II HCS Reader from Cellomics (Cellomics, PA, USA) has been described by Stiegler et al. [28]. Here, we describe measuring neurite outgrowth in LUHMES culture using a cell filling technique. While MAP2B immunocytochemistry has been used to image and quantify neurite growth in LUHMES cells [29], other studies have shown that the neurites extended by LUHMES cells express both dendritic and axonal properties [3]. Therefore, we generally use a cell filling technique to visualize neurites because it is quicker and less expensive.

To assay neurite growth and retraction in LUHMES cells:

- Detach LUHMES cells from the substrate with trypsinization 48 h after differentiation begins (day 2).

- Seed cells in 96-well plates at a density of 30,000 cells/well. Include both negative [cycloheximide (Sigma) at 3μM] and positive [p160ROCK inhibitor Y-27632 (Sigma) at 10μM] controls for neurite outgrowth in each 96-well plate [30]. These controls are most effective during the first 24 h after plating; when used later, they yield results that are more variable (Fig. 1).
- Chemical exposures can begin one or more hours after seeding as processes start to generate within hours after re-plating, which is optimal for assessing the effects of chemicals on initial neurite outgrowth.
- For neurite outgrowth exposures, prepare chemicals at twice the desired final concentration in tissue culture medium and add to each well at a volume equal to the volume of medium in the well (50μL) to minimize cell disruption.
- Remove the medium from each well 24 h later and replace it with 1× Dulbecco's PBS (with calcium and magnesium, ThermoFisher Scientific) containing 1μM calcein-AM, 1μg/mL Hoechst 33342 and 1.25μM PI.
- Incubate plates for 30 min at 37 °C while protected from light.
- Image the cells immediately after incubation. In live cells, calcein-AM is converted to a green fluorescent cytoplasmic product that fills the soma and neurites and can be observed using filters with ex/em spectra of 494/517 nm. Hoechst 33342, a nuclear dye, is imaged using ex/em 350/461 nm filters. PI labels dead cells and is imaged using ex/em 535/617 nm filters.

This protocol can be modified to measure neurite retraction at later times during differentiation by exposing cells to chemicals on day 5 (3 days after plating) via a complete exchange of media and imaging on day 6. Brefeldin-A (Millipore Sigma), an inhibitor of membrane trafficking, causes significant neurite retraction and is used as a positive control (at 10μM) for neurite retraction assays.

Chemical effects on neurite outgrowth can be influenced by plating surface, exposure time, and the method used for morphological analyses (Fig. 1). For example, 72, but not 48, h of exposure to PCB 95 (1 pM) increases neurite outgrowth in differentiated LUHMES cells plated on glass coverslips (*see* **Note 1**). Yet, neither a 72 nor a 48 h exposure to PCB 95 alters neurite outgrowth of LUHMES cells plated on tissue culture plastic. Moreover, the neurite growth promoting effects of PCB 95 were observed when cultures were immunostained for either MAP2B, a dendrite-selective cytoskeletal protein, or for phosphorylated neurofilaments, an axon-selective antigen, but not when using calcein-AM and Hoechst 33342. Since MAP2B is expressed only in more mature LUHMES cells, while neurites are extended by both mature and immature LUHMES cells [3], these data suggest that the

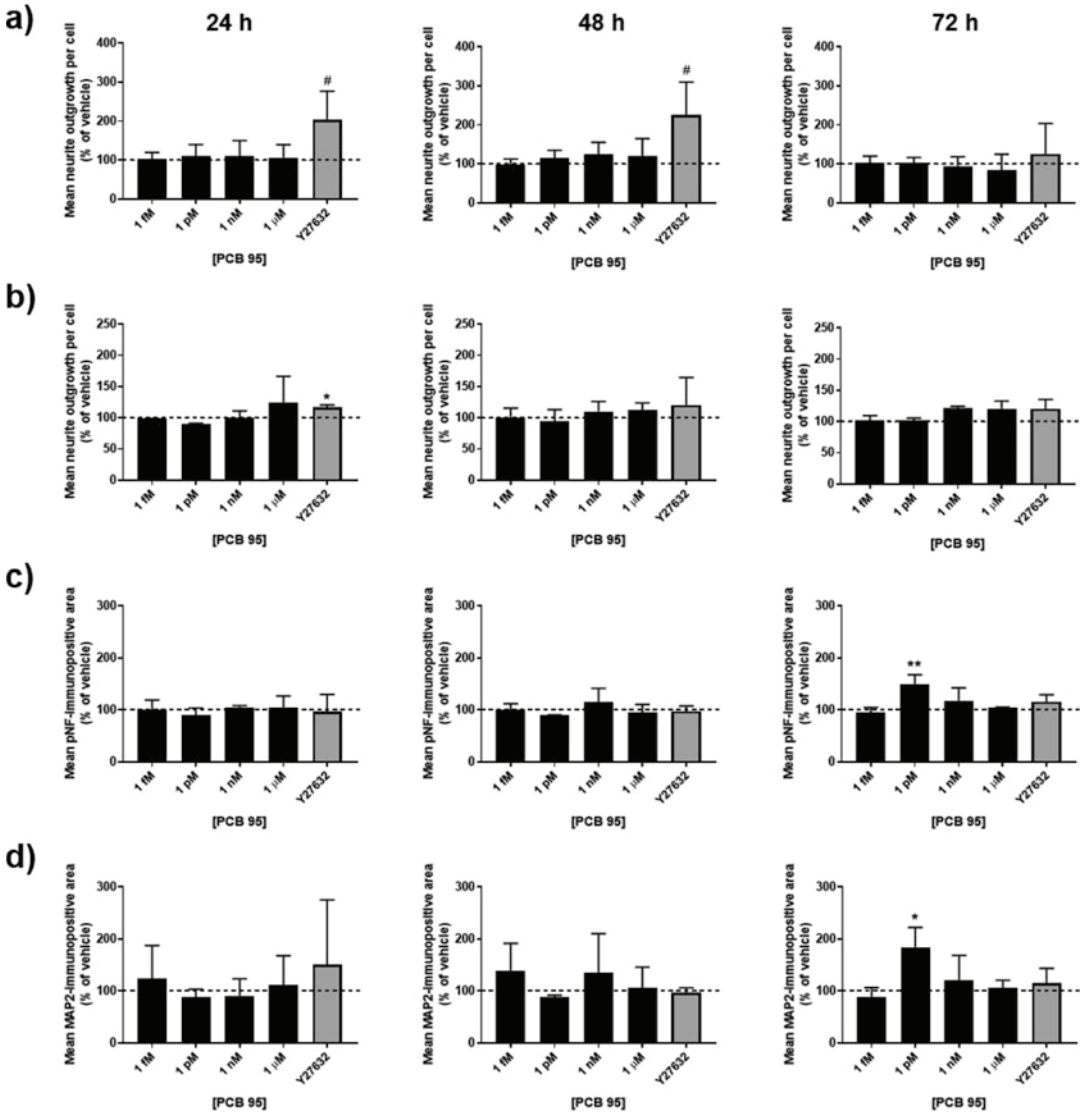


**Fig. 1** *Substrate, exposure time, and method of morphometric analysis influence outcome in cultured LUHMES cells, a human neuronal cell line.* (**a**, **b**) LUHMES cells at similar passage number were plated at the same cell density onto (**a**) tissue culture plastic or (**b**) glass coverslips and exposed to vehicle (0.1% DMSO) or varying concentrations of PCB 95 for 24, 48, or 72 h. Y-27632, a p160ROCK inhibitor that increases neurite outgrowth during the first 24 h after plating, was used as a positive control. (Note: as indicated in this Figure, when used at later times after plating, Y-27632 does not increase neurite outrgrowth). Neurite outgrowth was imaged by labeling cells with calcein-AM. (**c**, **d**) LUHMES cells grown on glass coverslips were exposed to vehicle or PCB 95 for 24–72 h, then immunostained for axons or dendrites using antibodies specific for (**c**) phosphorylated neurofilaments or (**d**) MAP2B, respectively. Data are presented as the mean $\pm$ SD ($n = 3$ independent experiments with eight wells in each experiment). *Significantly different from DMSO vehicle control at $p < 0.05$; **$p < 0.01$ as determined by one-way ANOVA with Dunnett's post hoc test; #significantly different from DMSO vehicle control as determined by Student's *t*-test

morphogenic effects of PCB 95 are manifest only at latter stages of neuronal differentiation. The observation that immunostaining for either a dendrite or axon-selective antigen yields the same outcome is consistent with the observation that the neurites extended by LUHMES cells exhibit both dendritic and axonal properties [3].

### 3.1.2 Labeling Axons Versus Dendrites in Dissociated Primary Sympathetic Neurons

Primary cultures of sympathetic neurons dissociated from the superior cervical ganglia (SCG) of laboratory rodents are a robust model system for assessing chemical effects on axonal or dendritic growth [17, 31]. SCG are easily accessible at varying life stages of rodents and yield a homogeneous neuronal cell population consisting of principal sympathetic neurons that can be maintained for weeks to months in serum-free defined culture medium in the absence or presence of ganglionic glial cells [31]. Primary sympathetic neurons extend a single process that is axonal within 24 h of plating, and this unipolar morphology can be sustained for up to 3 months when cultures are maintained in serum-free medium in the absence of glial cells [32, 33]. Robust dendritic growth can be induced in primary sympathetic neurons cultured in serum-free media by co-culturing them with ganglionic glial cells [34]. In sympathetic neurons grown in the absence of glial cells, dendritic growth can be triggered by the addition of recombinant BMP-2, 4, 6 or 7 (30–100 ng/mL; R&D Systems) or Matrigel (50–75μg/mL, Corning Life Sciences) to the culture medium [35]. The processes induced by BMPs and Matrigel appear about 48 h post-exposure, and exhibit functional, biochemical, and morphological characteristics of dendrites [33, 36].

The protocol for setting up primary sympathetic neurons from the SCG of perinatal rat or mouse pups on glass coverslips (ideal for morphometric analyses that can be done as early as 2 days in vitro (DIV)) has been published [35]. Protocols for immunostaining these cultures have also been published [37, 38] and are briefly described below:

- Fix cultures with 4% paraformaldehyde in 0.2 M phosphate buffer for 10 min at room temperature.
- Permeabilize cultures with 0.1% Triton-X-100 in PBS for 10 min at room temperature.
- Incubate cells in blocking buffer (PBS with 10% bovine serum albumin) for at least 1 h at room temperature.
- To identify axons, incubate cultures for 1 h at room temperature or overnight at 4 °C with Ab specific for phosphorylated NF-H and NF-M neurofilament subunits or Ab that recognizes synaptophysin. To visualize dendrites, incubate cultures with Ab specific for MAP2B or with Ab that recognizes dephosphorylated NF-H and NF-M. Dilute antibodies in blocking buffer (*see* **Note 2**).

- Remove excess primary antibody by rinsing the cultures three times with PBS over 5 min.
- Incubate with a fluorescent-tagged secondary antibody that recognizes the primary antibody for 1 h at room temperature or overnight at 4 °C in the dark.
- Remove excess secondary antibody by gently rinsing cultures three times with PBS over 5 min.
- If grown on glass coverslips, cultures are mounted cell side down in mounting medium on glass slides and the edges sealed with nail polish.
- If grown in multi-well plastic tissue culture plates, PBS containing DAPI is added to the well for 15 min, the wells rinsed twice with PBS, and the culture dish sealed with Parafilm™ to prevent evaporation until cultures are imaged.

### *3.1.3 Labeling Axons and Dendrites in Dissociated Cultures of Primary CNS Neurons*

Primary hippocampal and cortical neurons dissociated from perinatal rat or mouse pups are widely used in studies of neuronal morphogenesis and the effects of chemicals on axons and dendrites. In culture, these neurons exhibit a characteristic morphogenic program [39–41]. Stage 1 begins immediately after plating, when lamellipodia propagate around the somata signaling initial neurite formation. Growth cones develop in Stage 2 at the tips of neurites, enabling neurites to extend or retract short distances. Stage 2 lasts 12–36 h until one neurite begins to extend rapidly and its length exceeds that of the other "minor" neurites by 2- or 3-fold [40]. This single long neurite differentiates into the axon, while the other minor neurites slowly develop dendritic characteristics. As the culture ages, dendrites elongate and branch, and by approximately 21 DIV, synapses begin to form and dendritic spines appear [42]. This predictable morphogenic program makes primary hippocampal and cortical neurons a robust in vitro model for assessing chemical effects on axonal and dendritic morphologies of central neurons at varying stages of neuronal maturation.

Primary cortical and hippocampal neurons can be dissociated from embryonic day 18 or postnatal day 0 or 1 mouse or rat neocortices or hippocampi, as previously described [19, 43]. The former will contain significantly fewer glial cells than the latter. The neurons can be maintained at very low density for long periods of time using the "Banker" method of inverting the coverslip on which the neurons are plated over a monolayer of astrocytes [43]. Alternatively, cortical and hippocampal neurons can be cultured at high density in the presence of endogenous glia (mostly astrocytes) on the same coverslip [19]. With either method, cortical and hippocampal neurons develop a morphology that resembles that of their in vivo counterparts [20, 43]; however, we have found that the morphogenic response to neurotoxic chemicals can vary

depending on which culture method is used. In our experience, the chemical-induced morphogenic response of neurons cultured as high density neuron-glia co-cultures more closely resembles the response observed in vivo [14]. Additionally, the substrate on which the cells are plated can influence the morphogenic response to chemicals. Plating on glass coverslips is the best practice because lipophilic compounds, such as PCB 95, stick to plastic, which prevents or minimizes their effect on neuronal morphogenesis (Fig. 2).

To quantify axons in primary hippocampal or cortical cultures:

- Plate hippocampal or cortical neuron-glia co-cultures at 33,000 cells/cm$^2$.
- To quantify chemical effects on the complete axonal plexus of individual neurons, expose cells to vehicle or chemicals for 48 h beginning at 4 h post-plating [38].
- Fix cultures with 4% paraformaldehyde in 0.2 M phosphate buffer for 10 min at room temperature.
- Permeabilize cultures with 0.25% Triton-X-100 in PBS for 5 min at room temperature.
- Incubate cells in blocking buffer (PBS with 10% bovine serum albumin and/or 10% goat serum) for at least 1 h at room temperature or overnight at 4 °C.
- To identify axons, incubate cultures for 1 h at room temperature with Ab specific for tau-1. Dilute antibodies in blocking buffer (see Note 2).
- Remove excess primary antibody by rinsing the cultures three times with PBS over 5 min.
- Incubate with a fluorescent-tagged secondary antibody that recognizes the primary antibody for 1 h at room temperature or overnight at 4 °C in the dark.
- Remove excess secondary antibody by gently rinsing cultures two times with PBS over 5 min.
- If grown on glass coverslips, cultures are mounted cell side down in mounting medium on glass slides and the edges sealed with nail polish.
- If grown in multi-well plastic tissue culture plates, PBS containing Hoechst or DAPI is added to the well for 15 min, wells are rinsed twice with PBS, and the culture dish sealed with Parafilm™ to prevent evaporation until cultures are imaged.

To quantify dendritic arborization (total length, number of terminal tips, neurite mass, and number of branching points) in high density neuron-glia co-cultures, transfect a subpopulation of neurons (0.1–0.5%) with cDNA encoding a fluorescent protein:

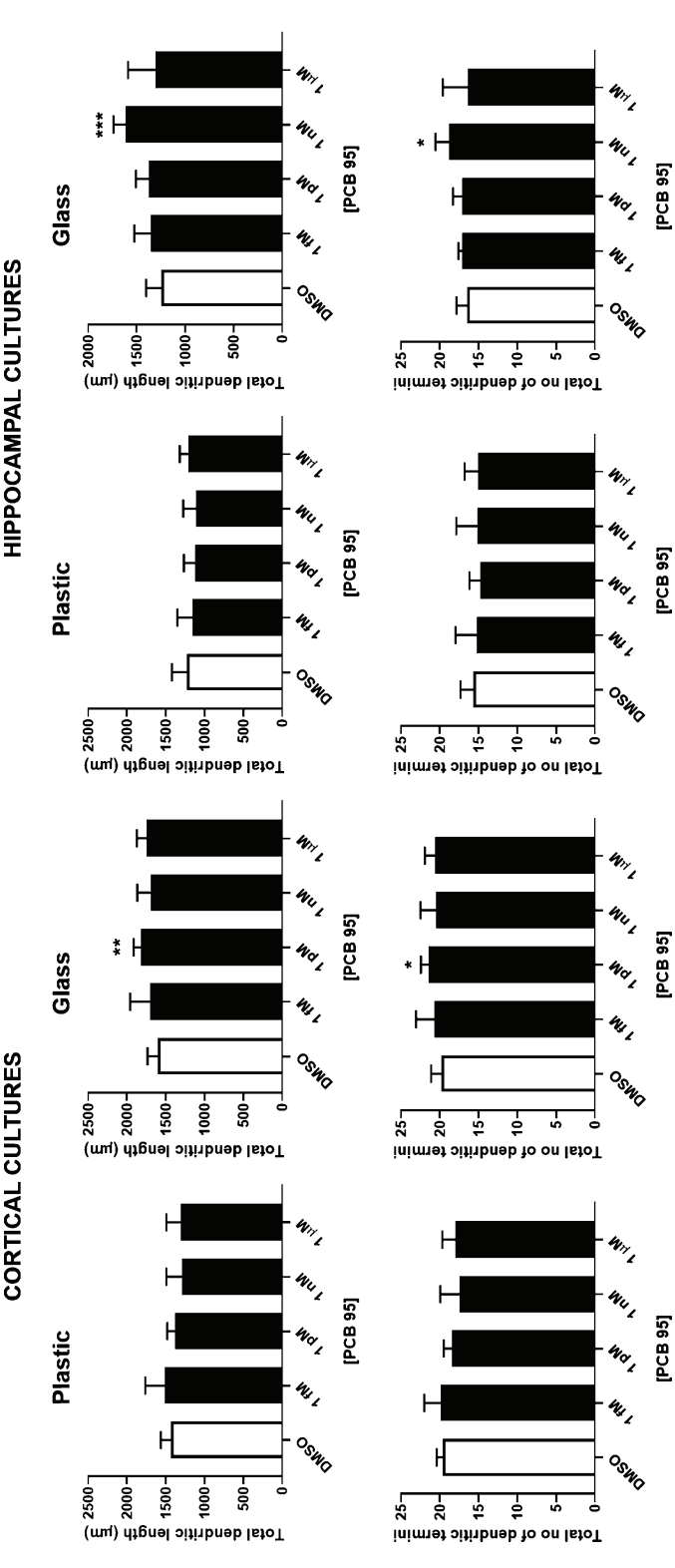


**Fig. 2** *Substrate composition influences morphogenic response of primary rat central neurons to neurotoxic agents.* Primary neuron-glia cultures dissociated from perinatal rat hippocampi and cortices were established at high density and maintained as previously described [19] on either tissue culture plastic or glass coverslips. At day in vitro (DIV) 6, cultures were transfected with cDNA encoding a MAP2B-eGFP construct to label the dendritic arbors of approximately 10% of the neurons in the culture. At DIV 7, cultures were exposed to vehicle (0.1% DMSO) or PCB 95 at varying concentrations for 48 h. Dendritic arborization was quantified in eGFP-positive cells (10–30 cells per well) as the total dendritic length and the total number of dendritic tips per neuron. Data are presented as the mean $\pm$ SD ($n = 5$–9 wells from three independent dissections). *Significantly different from DMSO vehicle control at $p < 0.05$; ** $p < 0.01$; *** $p < 0.001$ as determined by one-way ANOVA with Dunnett's post hoc test

- Dissociate cells from the neocortices or hippocampi of postnatal mice or rats. These can be sex segregated [44].
- Plate cells on glass coverslips at 83,000 cells/cm$^2$.
- At 4 DIV, treat cells with the anti-mitotic agent, cytosine arabinoside (Ara-C; Sigma) to curb glial cell proliferation by replacing 50% of the conditioned media with medium supplemented with 5μM Ara-C to yield a final Ara-C concentration of 2.5μM.
- The optimal window to assess the effects of chemicals on dendritic growth in high density neuron-glia co-cultures is between 4–10 DIV because this is the period of peak dendritic growth [20] although chemicals can be added to more mature cultures to assess effects on dendritic retraction.
- Transfect cells with plasmid encoding MAP2B-eGFP, MAP2B-FusRed, or pCAG-TFP [20] using Lipofectamine 2000 on DIV 6. Exceptions to the manufacturer's protocol include leaving the transfection solution on the cells for only 1–2 h and immediately replacing it at the end of the transfection period with conditioned media.
- On 7 DIV, treat cultures with vehicle or varying concentrations of test chemicals for 48–72 h [45].
- Fix cultures with 4% paraformaldehyde on 9 DIV and mount to glass slides using ProLong Gold Antifade reagent with DAPI (Thermo Fisher Scientific).

### *3.1.4 Ex Vivo Labeling of Dendritic Arbors in Peripheral Autonomic Ganglia Using Diolistics*

Diolistics uses pressure to deliver small beads coated with lipophilic carbocyanine dyes to stochastically label a subpopulation of cells within intact neural tissues [46]. The labeling of individual cells is rapid such that the entire dendritic arbor of neurons can be visualized within minutes after particles contact the cell membrane. This method is a variant of biolistics in which plasmids are delivered into hard-to-transfect cells, such as plant cells, by delivering small gold or tungsten particles coated with plasmids or other cDNA material using a gene gun. Diolistics was first described by Gan et al. [47] and uses fluorescent lipophilic dyes, such as DiI (1–1′-dioctade-cyl-3,3.3′,3′-tetramethylindocarbocyanine perchlorate, Thermo Fisher Scientific). Because of their lipophilic nature, these dyes partition into the plasma membrane, thereby outlining neuronal processes and spines. Membrane staining is more efficient and allows for better visualization of small thin protrusions than cytoplasmic staining. DiI-labeled neurons can be observed by high-resolution imaging, such as confocal or two-photon microscopy, and can be digitally reconstructed in precise detail [48, 49].

Our laboratory has used Diolistics to successfully label individual neurons in intact rat and mouse superior cervical ganglia (SCG) using the Helios® Gene Gun system from Bio-Rad [50]; we and

others have used this technique to label individual neurons in CNS organotypic slice cultures and cultured cells [20, 51]. The "bullets" used with the Helios gene gun are made of sections of Tefzel tubing filled with tungsten beads pre-coated with DiI.

To coat the Tefzel tubing with polyvinylpyrrolidone (PVP) (Sigma) to improve adherence of the tungsten beads to the interior walls of the tubing:

- Prepare a stock PVP solution at 20 mg/mL in 100% ethanol. Each day that bullets are prepared, the PVP solution is further diluted to 0.1 mg/mL in 100% ethanol.
- Cut approximately 30 inches of Tefzel tubing (Bio-Rad), rinse with 100% ethanol, and feed it into the Bio-Rad Prep station stopping just before the tubing enters the prep station gas outlet.
- Use a 10 mL syringe with a three-way stopcock mounted vertically on a ring stand next to the tubing prep station to avoid inserting air bubbles into the tubing and a short piece of silicone tubing to connect the stopcock to the Tefzel tubing.
- Pour the PVP solution into the syringe and open the stopcock to allow the PVP solution to fill the Tefzel tubing.
- Once the tubing is filled, close the stopcock to keep the PVP solution in the tubing for 5 min. Do not overfill the tubing and blot any excess with a Kimwipe™.
- Withdraw the PVP solution using the syringe.
- Gently push the Tefzel tubing into the gas outlet and connect it to the barbed hose connector on the prep station connected to a dry nitrogen gas source. Dry the tubing using a nitrogen gas rate of 0.4 L/min for approximately 5 min.

To prepare the tungsten particles:

- Suspend 15 mg of 1.1μm tungsten M-17 particles (Bio-Rad) in 150μL methylene chloride (99.9% pure, Fisher Scientific) in a 1.5 mL microfuge tube. Mix well and sonicate for 3 min to break up any bead clumps.
- Pipette the suspended particles onto a glass hanging drop slide and air dry for approximately 10–15 s to allow for even distribution of the particles.
- Place 3 mg of DiI in a microfuge tube, add 100μL of methylene chloride, and vortex.
- Pipette solution on top of the dried tungsten particles. Dried particles (<1 min) will appear as a dull gray powder. The edges of the hanging drop well where there is no tungsten will appear dark pink.

- Use a single edge razor blade to gently scrape the gray colored particles onto a piece of weigh paper, while avoiding the dark pink regions so as to not cause more clumping.
- Dice the particles into a fine powder and transfer to a 15 mL conical tube to which 5 ml of sterile MilliQ water is added.
- Vortex the tube containing the DiI-labeled beads in water for 30 s to allow larger particles to sink to the bottom of the tube. Do not sonicate because the dye will come off the particles.
- Place the vortexed particles in water in a new 10 mL syringe on the ring stand (a new syringe, stopcock, and silicone tubing should be used every time bullets are made).
- Open the stopcock and slowly push the dye-coated tungsten particle solution into the Tefzel tubing. Allow the particles to settle for 5 min. Leave the syringe connected to the tubing and do not rotate the tubing.
- Over a period of approximately 60 s, slowly remove the excess particles/water from the tubing with a syringe.
- Turn on the prep station motor to rotate the tubing and simultaneously dry it with nitrogen at a flow rate of 0.4 L/min for approximately 10–15 min for an even distribution of particles. As the water is removed, small droplets containing most of the particles will be left behind in the PVP-coated tube.
- Remove the tubing from the prep station and cut into 13-mm lengths using a tubing cutter.
- DiI bullets can be stored in a small scintillation type vial with a Dricap dehydrator cartridge (Sigma) in the dark for several weeks.

To label dendritic arbors:

- Harvest superior cervical ganglia from euthanized mice or rats (ranging in age from the first few weeks postnatal to adult animals), dissect the ganglia free from the capsule, and post-fix in 4% paraformaldehyde (Sigma) in 0.1 M phosphate buffer for 24 h at 4 °C.
- Transfer ganglia to PBS and store at 4 °C until use (best results are obtained with ganglia stored no more than 2–3 weeks).
- Load bullets into the bullet cartridge and assemble the gene gun per the manufacturer's instructions. The diameter of the initial barrel of the gun is approximately 1 cm and the extension barrel is 1.5 cm (the greatest density of particles will be within the 1-cm diameter when the gun is fired).
- Attach the gene gun to a helium source as the propellant. Helium is used because it is inert and disperses quickly after firing. Adjust the helium pressure depending on the species: 80–90 PSI for rat ganglia and 60 PSI for mouse ganglia.

- Place ganglia to be labeled in the center of a 60 mm petri dish previously prepared with a layer of Sylgard (Sylgard 184 silicone elastomer kit, Electron Microscopy Sciences, Hatfield PA, USA) and labeled with a hand-drawn 1 cm circle in the center of the bottom of the dish and a 1.5 cm circle around that. Sylgard acts as a shock absorber to help minimize tissue damage when the gun is fired.
- Blot excess PBS from the ganglia with a Kimwipe™.
- Put a 70μm cell strainer (Falcon, Corning NY, USA) over the end of the gun barrel to reduce clumping and disperse the particles.
- Hold the barrel approximately 1 cm over the ganglia and fire.
- Immediately rinse the ganglia in PBS, place them on a microscope slide in a drop of PBS, and image under fluorescent microscopy using an excitation filter of 568 nm to check labeling. If a dye-coated particle comes into contact with a neuron, it will begin to fill the cell with the dye. If there are no labeled neurons present, the same ganglia may be shot again up to 4–5 times until cells are labeled.

Usually, 2–3 neurons per ganglia will be labeled and can be imaged by confocal microscopy. Images should be acquired within 30 min of labeling to minimize dye diffusion into adjacent cells (*see* **Note 3**). Labeling that is too sparse or too dense to identify individual cellular components can be adjusted by changing the concentration of the particles in the solution that is loaded into the Tefzel tubing. If the dye appears clumped, fresh bullets may need to be made with special attention to ensure that the dye is evenly dispersed before loading into the tubing.

### 3.1.5 Golgi Staining

In 1873, Camillo Golgi discovered a technique that would impregnate nervous tissue with potassium dichromate and silver nitrate and randomly label only a limited number of neurons in a tissue, revealing the dendrites and axons extended by a single neuron. The mechanism by which this happens is still largely unknown, but the technique has become the gold standard for visualizing the complex dendritic arbors of central neurons in intact brain tissue.

In our laboratory, we use the Rapid Golgi staining method developed by Glaser and Van der Loos [52] to label pyramidal neurons in the rat and mouse hippocampus and cortex (*see* **Note 4**):

- Using the FD Rapid GolgiStain Kit (FD NeuroTechnologies, Inc.), prepare the Golgi solution 24 h prior to harvesting brains (approximately 14 mL total solution per rat brain). Mix solutions A and B at a 1:1 ratio in a 50 mL plastic conical tube protected from light at room temperature to allow settling of metal precipitate.

- 24 h later, add 7 mL of Golgi solution to individual 15 mL plastic tubes or scintillation vials to accommodate one brain hemisphere each. If using scintillation vials, remove the metal insert on the inside of the lid prior to use.
- After euthanasia, remove the fresh brain and gently drop into a petri dish filled with chilled PBS to rinse away excess blood.
- Bisect the brain using rectangular glass coverslips. Metal tools cannot be used with the Golgi solution.
- Using plastic forceps, gently transfer one whole hemisphere to a plastic tube/ scintillation vial containing the Golgi A + B solution (5 mL/$cm^3$ of tissue) and incubate overnight at room temperature in the dark (brain tissue should be protected from light at all times.)
- Using a plastic transfer pipette, remove the Golgi A + B solution after 24 h of incubation (discard as hazardous waste) and replace with 7 mL of fresh Golgi A + B solution.
- Incubate brains at room temperature for a total of 14 days, including the initial 24 h. Incubation for longer than 14 days will result in higher penetrance of the Golgi stain, increasing the likelihood of labeling neurons with overlapping dendritic arbors.
- After 14 days, remove the Golgi solution and add 7 mL of solution C. Incubate overnight at room temperature.
- The next day, remove solution C and replace with 7 mL of fresh solution C. Store the brain at 4 °C for 6 more days.
- Following this incubation period, transfer the brains to a new tube containing 10% sucrose in 0.1 M phosphate buffer, pH 7.2, at 4 °C.
- 24 h later, replace the 10% sucrose solution with 30% sucrose in the same buffer. Brains can be held in 30% sucrose for months in the dark at 4 °C, but use a similar duration of incubation for all brains in a given project to minimize the confounding effects of shrinkage that occurs over time.

To sub slides with gelatin and chromium potassium sulfate prior to sectioning brains:

- Heat 10 mg/mL gelatin solution in deionized water (400 mL) while stirring until the gelatin is dissolved.
- Add chromium potassium sulfate (1 mg/mL or 0.4 g for 400 mL) and stir to dissolve.
- Cool the solution to room temperature. Note: The solution can be filtered through a 60 cm Whatman #1 paper, but because this can take a long time and the solution often breaks through the paper cone, we often omit this step.

- Pour the solution into clean staining dishes containing clean slides in slide holders for 10 min. To avoid fingerprints, wear gloves and handle slides by their edges.
- Cover slides to prevent dust accumulation and dry overnight at room temperature.
- The remaining subbing solution can be refrigerated and used the next day to sub additional slides.

To section Golgi-stained brains with a Vibratome:

- Transfer Golgi-stained brains to 70% ethanol in a new plastic vial and keep at 4 °C for at least 4 h.
- Approximately 5 min before sectioning, cool the Vibratome basin to −20 °C.
- Remove the cerebellum and block the brain approximately 1 cm posterior to the olfactory bulb. Ensure the diameter of the brain cross-section is large enough to maintain tissue integrity during sectioning.
- Place the brain on a Kimwipe™ to remove excess ethanol on the face that was just blocked and glue (using Super Glue™) to the chuck with the cortex facing up. Keep the hippocampus above the glue to make the brain more stable. Allow the glue to harden for at least 5 min.
- Meanwhile, fill the Vibratome basin with ice-cold 70% ethanol with additional ice in the trough to keep the basin cool.
- Mount the chuck in the basin with the dorsal side of the brain facing the blade to reduce the force of the blade on the brain, which can break the glue and result in the brain cracking.
- Cut coronal sections of 100μm thickness and separate them from the whole brain using a paintbrush.
- Transfer sections to a petri dish containing cold solution C and allow each section to equilibrate until it is fully submerged.
- Transfer sections to subbed slides using a sterile transfer pipette with its tip cut off (to the wide diameter) so that suction can be applied to the whole brain slice. Note: Be sure to hold the cut tip pipette perpendicular to the petri dish and slide; otherwise, the entire volume of solution C may be ejected from the cut tip pipette onto the slide, resulting in shifting or loss of sections. For best results, move the section as close as possible to the pipette opening before transfer and keep parallel to the slide. Tap the cut tip pipette opening to the slide while gently ejecting a minimal volume. Ideally, there should be only a small volume of liquid covering the section. Alternatively, drops of solution C may be placed on the subbed slide, and once a slice has equilibrated in the petri dish of solution C, it can be moved with a paint brush tip to the subbed slide containing a light coating

layer of solution C. Once the sections are on the slide, aspirate the excess solution and add one to two drops of fresh solution C to each section.

- After 10 min, remove excess solution C with a Kimwipe™ laid flat on top of the section and very gently pull it off. This may need to be repeated once or twice.
- Loosely cover sections with foil to protect from dust and light and air dry at room temperature until no visible moisture remains. This may take weeks. Dab sections with a Kimwipe™ daily to accelerate the process.
- Brain slices will look opaque with no evidence of liquid once completely dried at which point they can be coverslipped in Permount™ (Sigma) mounting medium.

## 3.2 Imaging

### 3.2.1 Optimization of Fluorescent Image Quality

The reproducibility and rigor of quantitatively analyzing neurite outgrowth is highly dependent on image quality. Starting with high-quality samples is key to obtaining a high-quality image, and there are a number of steps common to every imaging system that if followed will help to greatly increase the sharpness (correct focus) and contrast (high signal to noise ratio) of thin structures like dendrites and axons. We use the ImageXpress high-content imaging system (Molecular Devices), which is interfaced to MetaXpress software (Molecular Devices), to acquire images from cell cultures or tissue sections that have been immunostained using fluorophore-tagged secondary antibodies. Most of the steps are part of the Plate Acquisition Setup, but the basic steps described below are conserved across almost all imaging software.

In the left panel of the Plate Acquisition Setup tab, there are subtabs that help guide imaging acquisition. Some of these subtabs are for entering and keeping a record of details of a project (Names and Description) and some are for directing the software to specific journals to be performed during (Journals) or after (Post-Acquisition) acquisition of the images for analysis. The subtabs that require attention and are common to any imaging software are:

- **Microscopic lens and camera:** Camera binning can be chosen here. Binning refers to the combination of the information of adjacent detectors in a camera sensor to create one single pixel in the recorded image. For example, a binning of two gathers the charges from a square of four detectors (two horizontal and two vertical) to record them in just one of the image pixels. Thus, the intensity per pixel increases by a factor of about four, increasing the signal-to-noise ratio, but reducing the resolution. The microscopic lens will also determine the resolution based on its magnification. Higher magnification reduces the field of view.

- **Plate, wells, and sites to visit:** The settings for the specific plate or slides is set here. The user can choose to avoid the edge wells if an "edge effect" is expected and choose the number and location of sites to image**.**
- **Acquisition loop**: Users can choose the number of wavelengths used to acquire the images and perform shading correction. The interaction between objects being imaged, the illumination and the camera can produce shading across the field-of-view. In some cases, there is a bright center and decreased brightness on the edges or it is darker on one side and lighter on the other. Precalibration with selected filters and objectives can minimize this shading effect.
- **Autofocus:** MetaXpress has different options of autofocus that are dependent on the type of plate used (usually 96-well plates work well with added z-focus around a fixed offset). More important than which autofocus is used, is applying it to multiple sites to ensure accuracy of the defined autofocus offset throughout the samples.
- **Wavelengths:** The time of exposure can be manually set or calculated in each wavelength by the software using the auto expose feature. To manually define the exposure time, different samples are used as positive controls (bright samples, usually cells of interest) and negative controls (dark samples, usually samples reacted with secondary Ab only) to keep the average image histogram in the lower 70% of exposure (target maximum intensity at about 45,000), and prevent image saturation that would lead to indistinguishable levels of labeling or dye concentration.
- **Save tiff images:** Images should be saved at the maximum bit depth of the camera used in the tiff format to maintain the highest resolution. Other formats compress the image and discard the image gradients that are important for analysis.

### *3.2.2 Imaging of Golgi-Stained Sections and Ganglia Labeled Using Diolistics*

The following describes how Golgi-stained sections and autonomic ganglia labeled with fluorescent dyes using Diolistics are selected and imaged on a confocal microscope in order to perform z-stacking:

- Visualize Golgi-stained sections under 10× magnification in brightfield to confirm staining is acceptable and identify suitable neurons.
- The brain region of interest must be clearly defined in the section (e.g., if analyzing pyramidal neurons in hippocampal CA1, sections should contain a clearly defined CA1 regions with highly aligned cell bodies (stratum pyramidale), distinguishable regions containing apical dendrites (stratum radiatum) and basilar dendrites (stratum origens)).

- Select individual neurons that: (1) are well-impregnated with no evidence of incomplete or artificial staining; (2) are not obscured by blood vessels, glia, or non-descript precipitate; (3) have a cell body located in the middle third of the thickness of the section; and (4) have a dendritic arbor clearly distinguishable from that of any adjacent labeled neurons. If a cell meets these criteria, the number of dendritic branches with cut ends should be ignored to prevent bias toward neurons with smaller dendritic arbors.
- When autonomic ganglia are labeled using Diolistics, select neurons for morphometric analysis if a tungsten particle is located within the cell body and the most distal aspects of the dendritic arbor are labeled as evidenced by tapering of fluorescence to very fine tips of dendritic processes.

Once neurons are identified that meet the inclusion criteria, sections are imaged at 20× magnification with a large enough z-stack to ensure complete capture of the dendritic arbors with the slice/ganglia:

- Track dendritic arbors out to the ends to ensure that arbors are visible in their entirety.
- Dendritic arbors may have breaks in them. If both ends of a broken primary dendrite are in close proximity in all planes, consider them connected. Do not consider dendrites connected if breaks are more than a couple microns or the ends are clearly not in the same z-plane. Broken secondary, tertiary, and quaternary dendrites are generally not considered connected unless there is overwhelming (proximity-based) evidence to suggest otherwise.
- Capture image stacks in brightfield for Golgi-stained sections and fluorescence for Diolistics using a 0.2μm z-step. Generally, 250–350 steps are necessary to capture an entire dendritic arbor of a hippocampal CA1 pyramidal neuron.
- Begin imaging at the lowest point where any dendrite is in focus and extend up to the highest point where any dendrite goes out of focus to ensure that all dendritic arbors in a field are visible and overlapping arbors can be differentiated.

It is recommended to capture images of six to eight neurons per brain from a minimum of six individual animal brains per experimental condition. Neurons can be traced using Neurolucida version 11 (MBF Bioscience, Willston, VT, USA), and Sholl analysis can be performed using Neurolucida Explorer. Help files are available in both platforms and online. Also available is NeuroMorpho.Org, which is "a centrally curated inventory of digitally reconstructed neurons associated with peer-reviewed publications that contains contributions from laboratories worldwide and is continuously updated." Morphometric analysis of Golgi-stained images

begins by manually outlining the cell body in Neurolucida and then manually tracing and marking dendrites. Manual tracing with Neurolucida is used to generate 3D Sholl plots, which can be exported into Excel files. For autonomic neurons labeled using Diolistics, three-dimensional images are reconstructed using Imaris software (Oxford Instruments) that are then compressed into two-dimensional images for morphometric analyses of dendritic lengths and somal diameter using NIH ImageJ.

### 3.3 Image Analysis

#### 3.3.1 High-Content Image Analysis and High-Throughput Screening

High-content image analysis is a technique in which fluorescent or transmission images of entire cells or cell organelles are simultaneously analyzed for multiple parameters [53]. In high-content screening, the extracted parameters are used to describe phenotypic changes elicited during screening of chemical libraries or sets [54]. High-content image analysis and screening are usually performed on automated high-content platforms, such as the ImageXpress (Molecular Devices), which allow users to image entire multiwell and slide formats to increase throughput while ensuring unbiased image acquisition. Image analysis can be performed directly during acquisition if the image analysis speed matches the acquisition speed or can be performed post-acquisition.

High-content screening of chemical effects on neurite outgrowth has been performed using the ToxCast library of chemicals [55] on many different cellular systems [24, 56–58]. While there are different software approaches available, both commercial and open source, they share similar image pre- and post-processing steps, the number of which is highly dependent on the in vitro or ex vivo system used in the study. The more complex the system, the more complex the image analysis, e.g., analyzing neurite outgrowth is less complex in pure neuronal cell cultures than in 3-D cell aggregates or tissue sections since the latter requires that neuronal cells first be isolated from other cell populations in the culture [59]. Cell density also influences the complexity of analysis as morphometric analysis on a single cell level is only feasible if the processes of each cell can be assigned to a given cell somata. This is why cell densities are often adjusted to lower values, which is not necessarily ideal for the overall health and survival of cells in culture, but represents a compromise between accuracy of morphometric analysis and cell viability [60]. Table 2 summarizes endpoints often measured in high-content screens of neurite outgrowth using various in vitro and in vivo systems.

While many endpoints, such as total process (neurite, axonal, or dendritic) length, number of terminal tips, number of branching points, neurite and process mass, soma area, and synaptic density can be analyzed using fully automated systems [28, 56, 57, 59–62], the same endpoints can be assessed semi-automatically in 3D-utilizing software like Neurolucida, but with some limitations.

**Table 2**
**High Content Screening (HCS) parameters that can be extracted from different in vitro and in vivo neuronal systems**

| Primary neuronal cell cultures | SY5Y, LUHMES, iPSCs | Neurospheres, organoid cultures, iPSCs-derived organoid cultures | Tissue section, cleared tissues imaged using CLARITY methodology |
|---|---|---|---|
| • Total neurite, axonal, and dendritic length<br>• Number of terminal tips<br>• Number of branching points<br>• Synaptic density<br>• Neurite, axonal, and dendritic mass<br>• Soma area<br>• Sholl analysis of dendritic or neuritic complexity | • Total neurite length<br>• Number of terminal tips<br>• Number of branching points<br>• Synaptic density<br>• Neurite, axonal, and dendritic mass<br>• Soma area | • Total neurite, axonal, and dendritic length<br>• Number of terminal tips<br>• Number of branching points<br>• Synaptic density<br>• Neurite, axonal, and dendritic mass<br>• Soma area | • Total neurite, axonal, dendritic length in 3D<br>• Number of terminal tips in 3D<br>• Number of branching points in 3D<br>• Synaptic density in 3D<br>• Neurite, axonal, dendritic mass in 3D<br>• Soma area in 3D<br>• Sholl analysis of dendritic or neuritic complexity in 3D |

Sholl analysis is another example of a common analysis usually performed in a semi-automated approach [44] (e.g., the Sholl Analysis plugin in ImageJ [63]).

The flow chart in Fig. 3 depicts the principal steps of assessing neurite outgrowth in LUHMES cell cultures with sample images depicted from the MetaXpress software (Molecular Devices). Figure 4 depicts a semi-automated Sholl analysis utilizing the Sholl analysis plugin in ImageJ [63], and Fig. 5 shows preliminary results of 3D fiber tracings of CGRP-stained nerve fibers in mouse bladder using Neurolucida 360 (MBF Bioscience).

#### 3.3.2 Image Preprocessing and Analysis

Acquired raw images of the nucleus and the biomarker used to identify processes (neurite, axon, or dendrite) are saved as 16 bit tiff images for further analysis. Most software for analyzing neurite outgrowth relies on dual-staining for nuclei and processes (neurites, axons, or dendrites). Cell nuclei are used to help identify cell somata and to separate cell soma that touch each other [59, 60, 64]. An exception is the widely used NeuronJ plugin [65] that allows the user to manually trace neurite structures by placing seeds on the image that are combined into lines by the software following the highest intensity gradient. Because this method is so tedious and time consuming, it is not suitable for screening assays.

Fluorescent images are almost exclusively converted into binary images through thresholding for consequent image segmentation (see Note 5). Thresholding aims to separate the raw image into two classes of pixels (foreground and background) and then computes the ideal threshold/intensity value to separate the two classes. If image intensities are comparable within a data set derived from a plate scanner with fixed exposure times and stained with the same antibody batch, a user-defined threshold can be set. The user defines foreground and background signal for the respective channels (Fig. 3b), and image information below this threshold is set to zero and only the foreground information (nuclei structures) is maintained. Since the signal-to-noise ratio for cell nuclei is usually very good, the fixed threshold method is robust among different experiments. In order to separate touching objects, a watershed segmentation [66] is performed (Fig. 3b), which separates touching cell nuclei. Henceforth, the image is treated as a surface with the height information encoded in the pixel intensity. The cell nuclei form catchment basins that are separated by the so-called watershed lines and can be used to separate the nuclei on the original image [67].

Somata identification is performed in a similar fashion as for nuclei and is required to separate processes from the neuronal cell body and assign processes to a single cell (*see* **Note 6**). Since the cell somata is usually much brighter than the cell processes [64], an initial high-fixed threshold value can be used to only maintain the

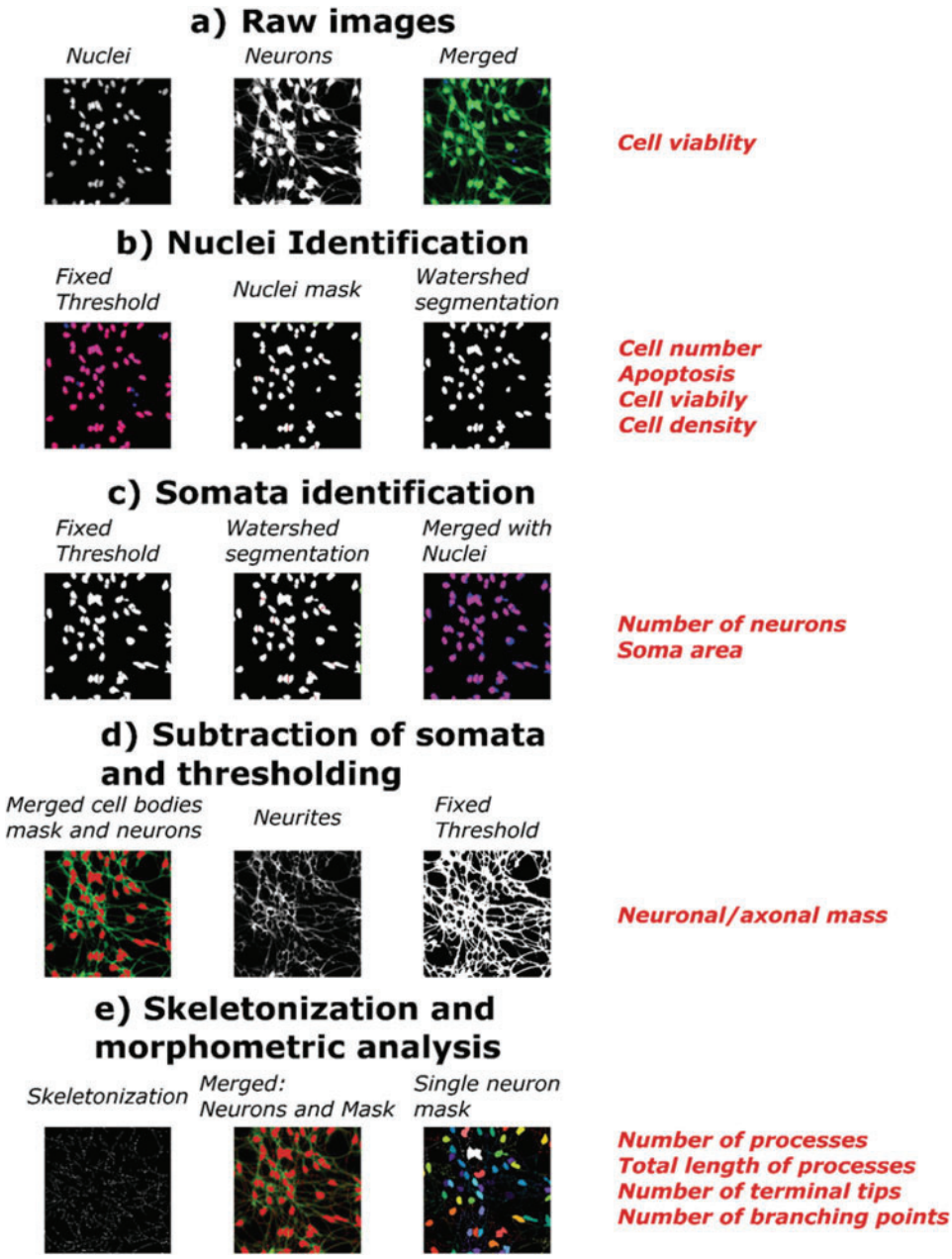


**Fig. 3** *High content analysis (HCA) workflow for morphometric analysis of LUHMES cells.* (***a***) Raw images of cell nuclei and neurons were acquired using an ImageXpress (Molecular Devices) high content imaging system and saved as 16 bit tiff files. Cell viability can be assessed by eye in the original images. (***b***) Cell nuclei are identified by applying a fixed threshold, followed by a watershed segmentation. The resulting binary mask of nuclei is used to determine cell number, cell density, and viability. Additionally, apoptosis can be assessed by counting bright cells with condensed chromatin. (***c***) Somata are identified by applying a fixed threshold on the original neuronal image, followed by a watershed segmentation. To further verify that the binary mask only contains neuronal somata, only areas containing a cell nucleus are considered to be neuronal somata. (***d***) In the next step, the neuronal somata are subtracted from the original image, and the remaining cellular

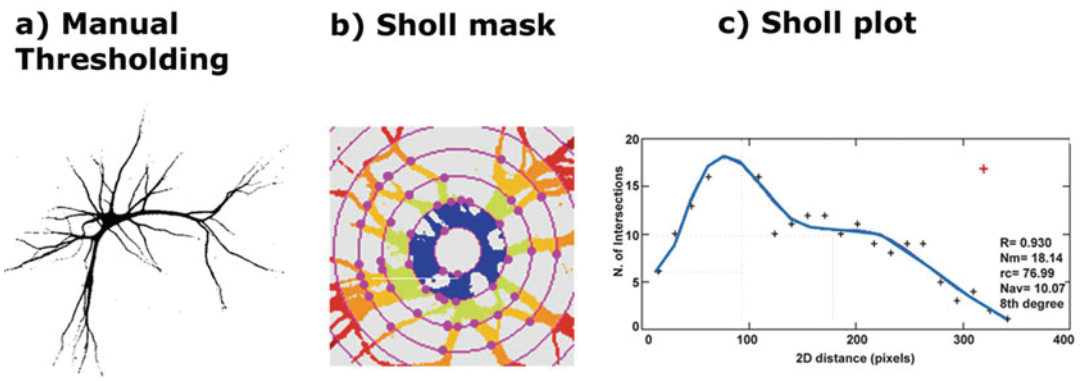


**Fig. 4** *Sholl analysis of dendritic arborization in primary rat cortical neuron-glia co-cultures.* (***a***) Dendrites of individual rat cortical neurons transfected with MAP2B-eGFP are manually thresholded, and a centroid is placed at the cell somata. (**b**) The Sholl analysis ImageJ plugin [63] automatically creates a Sholl mask by superimposing the binary image with concentric rings at user-defined distances from each other centered on the neuronal somata and counts the number of dendritic intersections on each ring (purple dots on the rings). (***c***) The number of dendritic intersections are graphed in a Sholl plot and saved as png and xlsx files

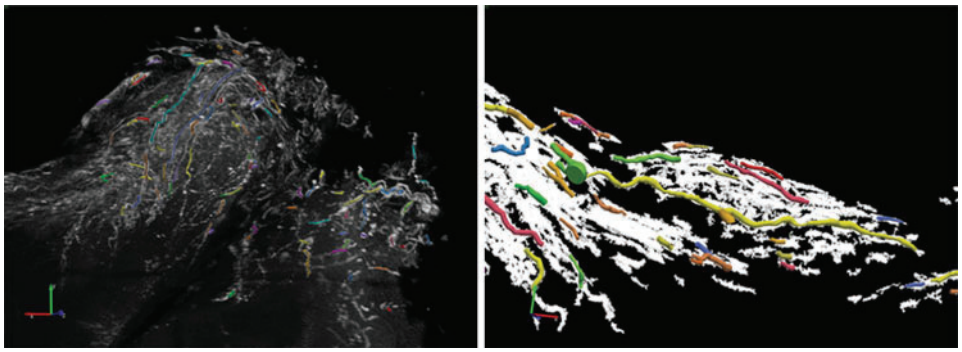

**Fig. 5** *Nerve fiber tracings in a rat bladder.* The left panel illustrates immunohistochemical staining for calcitonin gene-related peptide (CGRP) in an optically cleared section of the bladder wall of a young adult rat. Images were captured by multiphoton confocal microscopy using a CLARITY objective, and Neurolucida 360 software (MBP Biosciences) was used to automatically identify CGRP-immunopositive processes (color-coded surfaces). The right panel is a magnification of the same image

**Fig. 3** (continued) processes are thresholded with a value calculated from the remaining image, which is lower than the initial threshold to maintain dimly stained neurites. (***e***) Finally, the resulting binary mask of processes is skeletonized. A maximum width is set in order to only skeletonize neurites, which can now be attributed to single cells (colored binary mask). The number of neurites, total neurite length, number of terminal tips, and branching points can be assessed on a per cell basis. For high density cultures, often the total length and/or total number of neurites of the skeletonized image of the entire field of view is normalized against the total number of cells because an accurate assignment of neurites to individual neuronal cells is not feasible

brightest part of the neuron (Fig. 3c). Touching objects can be separated using watershed segmentation and resulting areas can be verified by checking if an area overlaps with the cell nuclei. There is higher user bias with fixed thresholds because different users will choose different thresholding values resulting in different morphometric results. Therefore, in high-content image analysis, automated methods like the Otsu method [68], which is based on separating image pixels into classes (foreground and background) by minimizing inter-class variance, are often used [64]. The Iterative Self-Organizing Data Analysis Technique (isodata method) is another widely used automated method [59, 69]. Automated methods provide the advantage of allowing for adjustments to varying signal-to-noise ratios in between different staining batches and eliminate user bias introduced in manual thresholding. The resulting binary image can be analyzed for neuron number and area of cell somata (Fig. 3c).

Verifying cell somata by checking for underlying nuclei delivers robust results for pure neuronal cultures, but it is prone to identifying false-positive nuclei in mixed in vitro cultures since in many cases neuron processes lay on top of non-neuronal cell bodies. This is particularly problematic for high density neuron-glia co-cultures and organoid cultures. In these cases, additional algorithms are required to reduce the false discovery rate while maintaining a high detection power. Such an approach is described for the Omnisphero software, which is designed to analyze neurite outgrowth in the neurosphere culture system [59]. When differentiated, the 3-D organoid system forms a high density heterogeneous cell layer from which neuronal cells have to be isolated from glia cells. This is accomplished by not only checking for overlap between nuclear and neurite processes markers, but also by verifying nuclei by checking their connectivity to adjacent neuronal processes [59].

Neuron somata are excluded from original neuron images to maintain only process structures (Fig. 3d). Processes are then skeletonized (Fig. 3e), which is a procedure that reduces a binary shape to a skeletal remnant, preserving what is equidistant to its boundaries. The skeleton usually resembles topological characteristics of the shape, such as connectivity, topology, and width. Skeletonization is used to quantify neurite/axonal/dendritic length, number of processes, number of branching points, and number of terminal tips from the binary masks. While there are many different skeletonization algorithms available [70], a common problem is the skeleton's sensitivity to an object's boundary deformation [70], and thresholding often results in imperfect object boundaries, which then introduce artificial branches within the skeleton. One solution is to limit the number of allowed vertices of endpoints [70]. However, this relies on a good characterization of the in vitro/in vivo

system because information on maximal number of end tips is required. In addition, while limiting the number of allowed endpoints in relatively immature neuronal cultures like LUHMES and neuronal progenitor cell-derived neurons [59], which are mainly bipolar with only a very low degree of branching, is feasible, this approach is not adequate for primary neuronal cell cultures. These cultures are comprised of different neuronal subtypes at different stages of maturation, which makes estimating maximal allowed endpoints challenging.

Another option is to post-process the obtained images in a pruning step that removes skeleton points that account for too high sensitivity. The two major pruning methods are based on significant measures assigned to each skeleton point and boundary smoothing algorithms performed on the original shape. The first method is often used to eliminate small branches originating from thresholding artifacts or artificial branching points. One method, described in [59], removes all branches from the skeleton and then checks the length of remaining sub-skeletons. Remaining sub-skeletons are reconnected and used for further analysis. This method removes artificial branching points as well as small branches originated from imperfect thresholding. Another method to describe denddritic structure is Sholl analysis [44]. This works well for mature primary hippocampal or cortical neurons. With this method, the user chooses individual neurons, defines a center point, and thresholds manually (Fig. 4a). The Sholl analysis plugin of ImageJ [63] superimposes concentric rings around the center point, determines the number of dendritic intersections at each ring, and generates a distribution plot (Fig. 4b, c). Because Sholl analysis is heavily dependent on the quality of thresholding, it is prone to thresholding biases from different researchers. Additionally, since it is only semi-automatic, it is not feasible for substance screening approaches. We recently published fully automated software for Sholl analysis that overcomes these limitations [62] by automatically determining thresholds, identifying cell somata, and correcting skeletons. This automated approach not only increases throughput, but also significantly reduces inter-researcher bias.

Analysis of dendritic and axonal morphology in the peripheral nervous system is mainly performed in a semi-automated fashion since nerve fibers have to be traced in 3D. Figure 5 shows automated fiber tracing results of Neurolucida 360 (MBF Bioscience). While some bright fibers are identified, the high auto-fluorescence background of the tissue prevents some fibers from being identified. However, auto-fluorescence can be subtracted by generating auto-fluorescence images derived from excitation wavelengths that are outside the used secondary antibody dyes. Furthermore, antibody penetration can be improved. This is a perfect example in which optimization of sample preparation and image acquisition

will improve the results. Once the final skeleton is obtained, total neurite length, number of processes, number of endpoints, number of terminal tips, and number of branching points can be assessed on a cellular level.

### 3.3.3 Data Validation Following Image Analysis

After images have been analyzed, the data are evaluated for validity. This is usually done via manual inspection of the obtained cell mask (Fig. 3e) in cultures exposed to reagents that inhibit neurite outgrowth [60]. Another option is to compare different methods (different image analysis software) to one another to confirm results are qualitatively similar or to compare the results to a gold standard, which is often considered to be manual tracing of neurites [71]. One of the most common features to be compared between the gold standard and the automated method is neuronal identification and quantification since this is a binary classification. A neuron is either correctly identified (true positive, TP); not identified (false negative, FN); correctly not identified, such as non-neuronal cells (true negatives, TN); or a non-neuronal cell is wrongly identified as a neuron (false positive, FP). For process length, the same holds true. However, length values will differ between automated and manual evaluations in all instances because while the computer computes process length from binary images, manual length measurements are performed on the original image. When comparing measurements made by automated versus manual methods, the relative change in positive and negative control values is often used to inform results.

The following equations can be used to determine the accuracy and precision of neuron identification:

$$\text{Accuracy} = \frac{\text{TP} + \text{TN}}{(\text{TP} + \text{TN} + \text{FP} + \text{FN})}$$

$$\text{Precision} = \frac{\text{TP}}{(\text{TP} + \text{FP})}$$

While both accuracy and precision can be used to determine the validity of an automated method, it is important to remember that low accuracy or precision values can result from low neuron identification or high FP identification. Therefore, the false discovery rate (FDR) and the detection power (DP) should be analyzed:

$$\text{FDR} = \frac{\text{FP}}{(\text{FP} + \text{TP})}$$

$$\text{DP} = \frac{\text{TP}}{(\text{TP} + \text{TN})}$$

These quantities are directly related to either identification quality or the false identification rate. However, the next question is: What are acceptable FDR and DP values? This question can be

answered by having two independent researchers analyze the same image set, with one researcher chosen as the "gold standard," and comparing the other researcher's results to this standard. The resulting FDR and DP may be considered as benchmark values [59]. See Tables 3 and 4 for open source and commercially available platforms (*see* **Note 7**).

## 4 Notes

1. ***Morphometric analysis of cultured neurons***: Neural cells should be plated on glass coverslips for analyses of chemical effects on neurite outgrowth. We have found that German glass coverslips yield the most reproducible effects. In addition, we strongly advise that researchers consider whether the chemical properties of test compounds favor adsorption to tissue culture plastic or to glass.
2. ***Visualizing axons* vs. *dendrites by immunocytochemistry:*** It is critically important that axon and dendrite-selective antibodies be carefully titered prior to experimentation to ensure specificity of staining. If used at too high of a concentration, many of these antibodies will non-selectively label processes (e.g., at too high of a concentration, antibodies specific for MAP2B will label axons in addition to dendrites).
3. ***Diolistics:*** The lipophilic dyes coated on the tungsten beads spread very quickly into the cell membrane, labeling cells within minutes. With time, this dye will spread to adjacent cells, so it is critical that you have access to imaging equipment while you are labeling cells. If you wait more than several hours to image after labeling, it will become difficult to distinguish the dendritic arbor of an individual neuron from that of adjacent cells.
4. ***Golgi staining:*** In our hands, we have not had much success using the FD Rapid GolgiStain Kit to label central neurons in the brains of embryonic or early postnatal mice and rats. Postnatal day 21 is the earliest that we have been able to successfully Golgi stain brains using this particular kit. We have also not had much success in using the FD Rapid GolgiStain kit to label neurons in autonomic ganglia. Please note that the metals used in the Golgi stain stick to many surfaces. In particular, if you use your vibratome for applications in addition to Golgi staining, it is advisable to have a separate blade and basin reserved exclusively for processing Golgi-stained brains.
5. ***Imaging: Thresholding.*** Thresholding results are highly dependent on the signal-to-noise ratio and are thus dependent on image quality. In many cases, optimization of image quality

**Table 3**
**Examples of open source software packages and their applicability for analyzing various morphological features of differentiated neurons**

| Tool | Software platform | Total neurite length | Total axonal length | Total dendritic length | Number of terminal tips | Number of branching points | Synapse density | Neurite Mass | Axonal Mass | Dendritic Mass | Cell body area | Sholl analysis |
|---|---|---|---|---|---|---|---|---|---|---|---|---|
| NeuronJ, AnalyzeSkeleton SYNAPCOUNTJ Sholl Analysis [63] | ImageJ | + | + | + | + | + | + | + | + | + | + | + |
| GAIN [64] | MATLAB | ++ | ++ | ++ | – | – | – | – | – | – | – | – |
| NeuronCyto II [73] | MATLAB | ++ | ++ | ++ | – | ++ | – | – | – | – | ++ | – |
| Omnisphero [59, 62] | MATLAB | ++ | ++ | ++ | ++ | ++ | ++ | ++ | ++ | ++ | ++ | ++ |
| NeuriteQuant [74] | ImageJ | ++ | ++ | ++ | ++ | ++ | – | – | – | – | ++ | |

– Not available, + Manual or semi-automatic, ++ Fully automated

**Table 4**
**Examples of commercial software packages and their usefulness for analyzing various morphological features of differentiated neurons**

| Tool | Software Platform | Total neurite length | Total axonal length | Total dendritic length | Number of terminal tips | Number of branching points | Synapse density | Neurite Mass | Axonal Mass | Dendritic Mass | Cell body area | Sholl analysis |
|---|---|---|---|---|---|---|---|---|---|---|---|---|
| Neurite Outgrowth Assay [60] Synaptogenesis Assay [75] | HCS Studio 2.0 (Thermo Fisher) | ++ | ++ | ++ | ++ | ++ | ++ | ++ | ++ | ++ | ++ | – |
| MetaXpress 5 | Molecular Devices | ++ | ++ | ++ | ++ | ++ | ++ | ++ | ++ | ++ | ++ | – |
| Neurolucida Neurolucida 360 [76] | Neurolucida | + | + | + | + | + | + | + | + | + | + | + |

– Not available, + Manual or semi-automatic, ++ Fully automated

is the most important step. Image quality is highly dependent on the optical system. The higher the resolution and the lower the noise of the detector, the easier the analysis of images. This, however, will sometimes come at the cost of longer acquisition time, thus slowing down screening approaches. When fixed optical systems are used, the algorithms can be made more robust by using deep learning approaches for image semantic segmentation. In order to do so, masks of correctly segmented neurons would be used to train convolution neuronal networks. During training, image augmentation can be introduced to generalize brightness and contrast fluctuations. Image augmentation will artificially alter image brightness and contrast so that the algorithms become more robust. Of note, deep learning approaches require training images in the range of 1000–2000 depending on the difficulty of the task (variation within the training data, such as brightness variations and artifacts like bubbles), which will require a high manual workload on checking masks. To reduce the time to generate training masks, it is common practice to refine masks obtained by classic thresholding methods. Using this approach, only some pixels need to be deleted or added rather than annotating the entire cell. Thresholding methods can vary for different systems, and available options should be examined prior to establishing a new analysis pipeline. It is important to test the thresholding method on non-stained samples and controls reacted with only secondary antibody to ensure nonspecific signal is not detected. A complete new thresholding algorithm might be needed for classical image analysis. In contrast, neuronal networks can be retrained with the new images, by refining masks obtained from the initial segmentation of the network by a researcher (filling or deleting parts of the mask).

6. ***Imaging:*** Cellular morphology requires the assignment of processes to a given cell somata. While this works well for low density cell cultures, assignment in high density cultures is not feasible due to the high intersection of processes from different cells. In this case, the more accurate approach is to normalize the total skeleton length to the number of identified cell somata. Another option is to use transfection agents with low transfection efficiency so that the density of labeled cells is low.
7. ***Imaging:*** Tables 3 and 4 give an overview of some open source and commercially available software platforms and their endpoint spectra.

## Acknowledgments

The authors thank Dr. Suzette Smiley-Jewell (University of California, Davis) for reviewing and editing the manuscript. This work was funded by the National Institute of Aging (R01 AG056710), the National Institute of Child Health and Human Development (P50 HD103526), and the National Institute of Environmental Health Sciences (R01 ES014901).

### References

1. Lasek R (1988) Studying the intrinsic determinants of neuronal form and function. In: Lasek R, Black MB (eds) Intrinsic determinants of neuronal form and function. A.R. Liss, New York, pp 3–58
2. Higgins D, Burack M, Lein P, Banker G (1997) Mechanisms of neuronal polarity. Curr Opin Neurobiol 7:599–604
3. Scholz D, Poltl D, Genewsky A, Weng M, Waldmann T et al (2011) Rapid, complete and large-scale generation of post-mitotic neurons from the human LUHMES cell line. J Neurochem 119:957–971
4. Berger-Sweeney J, Hohmann CF (1997) Behavioral consequences of abnormal cortical development: insights into developmental disabilities. Behav Brain Res 86:121–142
5. Cremer H, Chazal G, Goridis C, Represa A (1997) NCAM is essential for axonal growth and fasciculation in the hippocampus. Mol Cell Neurosci 8:323–335
6. Maier DL, Mani S, Donovan SL, Soppet D, Tessarollo L et al (1999) Disrupted cortical map and absence of cortical barrels in growth-associated protein (GAP)-43 knockout mice. Proc Natl Acad Sci U S A 96:9397–9402
7. Rice D, Barone S Jr (2000) Critical periods of vulnerability for the developing nervous system: evidence from humans and animal models. Environ Health Perspect 108(Suppl 3):511–533
8. Copf T (2016) Impairments in dendrite morphogenesis as etiology for neurodevelopmental disorders and implications for therapeutic treatments. Neurosci Biobehav Rev 68:946–978
9. Engle EC (2010) Human genetic disorders of axon guidance. Cold Spring Harb Perspect Biol 2:a001784
10. Garey L (2010) When cortical development goes wrong: schizophrenia as a neurodevelopmental disease of microcircuits. J Anat 217:324–333
11. Penzes P, Cahill ME, Jones KA, VanLeeuwen JE, Woolfrey KM (2011) Dendritic spine pathology in neuropsychiatric disorders. Nat Neurosci 14:285–293
12. Robichaux MA, Cowan CW (2014) Signaling mechanisms of axon guidance and early synaptogenesis. Curr Top Behav Neurosci 16:19–48
13. Supekar K, Uddin LQ, Khouzam A, Phillips J, Gaillard WD et al (2013) Brain hyperconnectivity in children with autism and its links to social deficits. Cell Rep 5:738–747
14. van Thriel C, Westerink RH, Beste C, Bale AS, Lein PJ et al (2012) Translating neurobehavioural endpoints of developmental neurotoxicity tests into in vitro assays and readouts. Neurotoxicology 33:911–924
15. Stamou M, Streifel KM, Goines PE, Lein PJ (2013) Neuronal connectivity as a convergent target of gene x environment interactions that confer risk for autism spectrum disorders. Neurotoxicol Teratol 36:3–16
16. Costa LG (2017) Overview of neurotoxicology. Curr Protoc Toxicol 74:11.1.1–11.1.11
17. Howard AS, Bucelli R, Jett DA, Bruun D, Yang D et al (2005) Chlorpyrifos exerts opposing effects on axonal and dendritic growth in primary neuronal cultures. Toxicol Appl Pharmacol 207:112–124
18. Yang D, Kania-Korwel I, Ghogha A, Chen H, Stamou M et al (2014) PCB 136 atropselectively alters morphometric and functional parameters of neuronal connectivity in cultured rat hippocampal neurons via ryanodine receptor-dependent mechanisms. Toxicol Sci 138:379–392
19. Sethi S, Keil KP, Chen H, Hayakawa K, Li X et al (2017) Detection of 3,3'-dichlorobiphenyl in human maternal plasma and its effects on axonal and dendritic growth in primary rat neurons. Toxicol Sci 158:401–411
20. Wayman GA, Impey S, Marks D, Saneyoshi T, Grant WF et al (2006) Activity-dependent

dendritic arborization mediated by CaM-kinase I activation and enhanced CREB-dependent transcription of Wnt-2. Neuron 50:897–909

21. Cai D, Cohen KB, Luo T, Lichtman JW, Sanes JR (2013) Improved tools for the Brainbow toolbox. Nat Methods 10:540–547
22. Chung K, Wallace J, Kim SY, Kalyanasundaram S, Andalman AS et al (2013) Structural and molecular interrogation of intact biological systems. Nature 497:332–337
23. Feng G, Mellor RH, Bernstein M, Keller-Peck C, Nguyen QT et al (2000) Imaging neuronal subsets in transgenic mice expressing multiple spectral variants of GFP. Neuron 28:41–51
24. Radio NM, Mundy WR (2008) Developmental neurotoxicity testing in vitro: models for assessing chemical effects on neurite outgrowth. Neurotoxicology 29:361–376
25. Delp J, Funke M, Rudolf F, Cediel A, Bennekou SH et al (2019) Development of a neurotoxicity assay that is tuned to detect mitochondrial toxicants. Arch Toxicol 93:1585–1608
26. Matelski L, Morgan RK, Grodzki AC, Van de Water J, Lein PJ (2021) Effects of cytokines on nuclear factor-kappa B, cell viability, and synaptic connectivity in a human neuronal cell line. Mol Psychiatry 26:875–887
27. Lotharius J, Barg S, Wiekop P, Lundberg C, Raymon HK et al (2002) Effect of mutant alpha-synuclein on dopamine homeostasis in a new human mesencephalic cell line. J Biol Chem 277:38,884–38,894
28. Stiegler NV, Krug AK, Matt F, Leist M (2011) Assessment of chemical-induced impairment of human neurite outgrowth by multiparametric live cell imaging in high-density cultures. Toxicol Sci 121:73–87
29. Ilieva M, Della Vedova P, Hansen O, Dufva M (2013) Tracking neuronal marker expression inside living differentiating cells using molecular beacons. Front Cell Neurosci 7:266
30. Roloff F, Scheiblich H, Dewitz C, Dempewolf S, Stern M et al (2015) Enhanced neurite outgrowth of human model (NT2) neurons by small-molecule inhibitors of rho/ROCK signaling. PLoS One 10: e0118536
31. Lein PJ, Fryer AD, HIggins D (2009) Cell culture: autonomic and enteric neurons. In: Squire LR (ed) Encyclopedia of neuroscience. Academic Press, Oxford, pp 625–632
32. Bruckenstein DA, HIggins D (1988) Morphological differentation of embryonic rat sympathetic neurons in tissue culture I. Conditions under which neurons form axons but not dendrites. Dev Biol 136:324–336
33. Lein PJ, Higgins D (1989) Laminin and a basement membrane extract have different effects on axonal and dendritic outgrowth from embryonic rat sympathetic neurons in vitro. Dev Biol 136:330–345
34. Tropea M, Johnson MI, Higgins D (1988) Glial cells promote dendritic development in rat sympathetic neurons in vitro. Glia 1:380–392
35. Ghogha A, Bruun DA, Lein PJ (2012) Inducing dendritic growth in cultured sympathetic neurons. J Vis Exp (61):3546. https://doi.org/10.3791/3546
36. Lein P, Johnson M, Guo X, Rueger D, Higgins D (1995) Osteogenic protein-1 induces dendritic growth in rat sympathetic neurons. Neuron 15:597–605
37. Lein PJ (1991) The NC1 domain of type IV collagen promotes axonal growth in sympathetic neurons through interaction with the alpha 1 beta 1 integrin. J Cell Biol 113:417–428
38. Lein PJ, Guo X, Shi GX, Moholt-Siebert M, Bruun D et al (2007) The novel GTPase Rit differentially regulates axonal and dendritic growth. J Neurosci 27:4725–4736
39. Dotti CG, Sullivan CA, Banker GA (1988) The establishment of polarity by hippocampal neurons in culture. J Neurosci 8:1454–1468
40. Goslin K, Banker G (1989) Experimental observations on the development of polarity by hippocampal neurons in culture. J Cell Biol 108:1507–1516
41. Goslin K, Banker G (1990) Rapid changes in the distribution of GAP-43 correlate with the expression of neuronal polarity during normal development and under experimental conditions. J Cell Biol 110:1319–1331
42. Fletcher TL, Banker G (1989) The establishment of polarity by hippocampal neurons: the relationship between the stage of a cell's development in situ and its subsequent development in culture. Dev Biol 136:446–454
43. Kaech S, Banker G (2006) Culturing hippocampal neurons. Nat Protoc 1:2406–2415
44. Keil KP, Sethi S, Wilson MD, Chen H, Lein PJ (2017) In vivo and in vitro sex differences in the dendritic morphology of developing murine hippocampal and cortical neurons. Sci Rep 7:8486
45. Wayman GA, Bose DD, Yang D, Lesiak A, Bruun D et al (2012) PCB-95 modulates the calcium-dependent signaling pathway

responsible for activity-dependent dendritic growth. Environ Health Perspect 120:1003–1009

46. Grutzendler J, Tsai J, Gan WB (2003) Rapid labeling of neuronal populations by ballistic delivery of fluorescent dyes. Methods 30:79–85
47. Gan WB, Grutzendler J, Wong WT, Wong RO, Lichtman JW (2000) Multicolor "DiOlistic" labeling of the nervous system using lipophilic dye combinations. Neuron 27:219–225
48. O'Brien JA, Holt M, Whiteside G, Lummis SC, Hastings MH (2001) Modifications to the hand-held gene gun: improvements for in vitro biolistic transfection of organotypic neuronal tissue. J Neurosci Methods 112:57–64
49. Noterdaeme M, Mildenberger K, Minow F, Amorosa H (2002) Evaluation of neuromotor deficits in children with autism and children with a specific speech and language disorder. Eur Child Adolesc Psychiatry 11:219–225
50. Kim WY, Gonsiorek EA, Barnhart C, Davare MA, Engebose AJ et al (2009) Statins decrease dendritic arborization in rat sympathetic neurons by blocking RhoA activation. J Neurochem 108:1057–1071
51. Seabold GK, Daunais JB, Rau A, Grant KA, Alvarez VA (2010) DiOLISTIC labeling of neurons from rodent and non-human primate brain slices. J Vis Exp (41):2081. https://doi.org/10.3791/2081
52. Glaser EM, Van der Loos H (1981) Analysis of thick brain sections by obverse-reverse computer microscopy: application of a new, high clarity Golgi-Nissl stain. J Neurosci Methods 4:117–125
53. Haney S (2008) High content screening: science, techniques and applications. Wiley Online Library
54. Gasparri F (2009) An overview of cell phenotypes in HCS: limitations and advantages. Expert Opin Drug Discov 4:643–657
55. Radio NM, Breier JM, Reif DM, Judson RS, Martin M et al (2015) Use of neural models of proliferation and neurite outgrowth to screen environmental chemicals in the ToxCast phase I library. In: McKim JM (ed) Applied in vitro toxicology. Mary Ann Liebert, Inc.
56. Anderl JL, Redpath S, Ball AJ (2009) A neuronal and astrocyte co-culture assay for high content analysis of neurotoxicity. J Vis Exp (27):1173. https://doi.org/10.3791/1173
57. Harrill JA, Freudenrich TM, Robinette BL, Mundy WR (2011) Comparative sensitivity of human and rat neural cultures to chemical-induced inhibition of neurite outgrowth. Toxicol Appl Pharmacol 256:268–280
58. Radio NM, Freudenrich TM, Robinette BL, Crofton KM, Mundy WR (2010) Comparison of PC12 and cerebellar granule cell cultures for evaluating neurite outgrowth using high content analysis. Neurotoxicol Teratol 32:25–35
59. Schmuck MR, Temme T, Dach K, de Boer D, Barenys M et al (2017) Omnisphero: a high-content image analysis (HCA) approach for phenotypic developmental neurotoxicity (DNT) screenings of organoid neurosphere cultures in vitro. Arch Toxicol 91:2017–2028
60. Harrill JA, Freudenrich TM, Machacek DW, Stice SL, Mundy WR (2010) Quantitative assessment of neurite outgrowth in human embryonic stem cell-derived hN2 cells using automated high-content image analysis. Neurotoxicology 31:277–290
61. Harrill JA, Robinette BL, Freudenrich T, Mundy WR (2013) Use of high content image analyses to detect chemical-mediated effects on neurite sub-populations in primary rat cortical neurons. Neurotoxicology 34:61–73
62. Schmuck MR, Keil KP, Sethi S, Morgan RK, Lein PJ (2020) Automated high content image analysis of dendritic arborization in primary mouse hippocampal and rat cortical neurons in culture. J Neurosci Methods 341:108793
63. Ferreira TA, Blackman AV, Oyrer J, Jayabal S, Chung AJ et al (2014) Neuronal morphometry directly from bitmap images. Nat Methods 11:982–984
64. Long BL, Li H, Mahadevan A, Tang T, Balotin K et al (2017) GAIN: a graphical method to automatically analyze individual neurite outgrowth. J Neurosci Methods 283:62–71
65. Meijering E, Jacob M, Sarria JC, Steiner P, Hirling H et al (2004) Design and validation of a tool for neurite tracing and analysis in fluorescence microscopy images. Cytometry A 58:167–176
66. Roerdink JBTM, Meijster A (2000) The watershed transform: definitions, algorithms and parallelization strategies. Fundamenta Informaticae 41:187–228
67. Gonzalez RC, Woods RE (2008) Digital image processing. Prentice Hall Inc., Upper Saddle River, NJ
68. Otsu N (1979) A threshold selection method from gray-level histograms. EEE Trans Syst Man Cybern 9:62–66
69. Ridler TW (1978) Picture thresholding using an iterative selection method. IEEE Trans Syst Man Cybern 8:630–632

70. Bai X, Latecki LJ, Liu WY (2007) Skeleton pruning by contour partitioning with discrete curve evolution. IEEE Trans Pattern Anal Mach Intell 29:449–462
71. Versi E (1992) "Gold standard" is an appropriate term. BMJ 305:187
72. Blacklock AD, Cauveren JA, Smith PG (2004) Estrogen selectively increases sensory nociceptor innervation of arterioles in the female rat. Brain Res 1018:55–65
73. Ong KH, De J, Cheng L, Ahmed S, Yu W (2016) NeuronCyto II: an automatic and quantitative solution for crossover neural cells in high throughput screening. Cytometry A 89:747–754
74. Dehmelt L, Poplawski G, Hwang E, Halpain S (2011) NeuriteQuant: an open source toolkit for high content screens of neuronal morphogenesis. BMC Neurosci 12:100
75. Harrill JA, Robinette BL, Mundy WR (2011) Use of high content image analysis to detect chemical-induced changes in synaptogenesis in vitro. Toxicol In Vitro 25:368–387
76. Abate G, Colazingari S, Accoto A, Conversi D, Bevilacqua A (2018) Dendritic spine density and EphrinB2 levels of hippocampal and anterior cingulate cortex neurons increase sequentially during formation of recent and remote fear memory in the mouse. Behav Brain Res 344:120–131

# Part II

## Physiological Evaluation in Rodents